Ab initio Computational Insight into the Interaction of Alkyl-substituted Ethene and Sulfenyl Halide

Ausra Vektariene and Gytis Vektaris

Vilnius University Institute of Theoretical Physics and Astronomy, A. Gostauto 12, 01108 Vilnius, Lithuania

Reprint requests to Dr. A. Vektariene.
E-mail: ausra.vektariene@gmail.com or ausra.vektariene@tfai.vu.lt

Z. Naturforsch. **2011**, *66b,* 850 – 856; received April 18, 2011

The *ab initio* calculations approach was used to determine the mechanism of interaction between propene and a sulfenyl halide. The second-order Møller-Plesset corrections for the electron correlation energy were applied to calculate the most probable Gibbs Free Energy profiles for the selected reaction. All optimized structures were confirmed by vibrational frequency analysis and intrinsic reaction coordinate calculations. Two possible reaction pathways were proposed and evaluated to conclusively characterize the reaction. The reaction proceeds *via* formation of a cyclic episulfonium intermediate, stereoselective ring opening of the episulfonium intermediate by the chloride anion, and isomerization of the adduct of the kinetically controlled reaction into the thermodynamically favorable product.

Key words: Quantum Chemical Calculations, Gibbs Free Energy Profile, Addition Reaction

Introduction

Electrophilic additions of sulfenyl halides to alkenes have been extensively studied since 1960 [1 – 15]. However, many aspects of their mechanisms have not been fully disclosed.

It is known that the reaction exhibits high regioselectivity and stereoselectivity [4 – 15]. The reaction progresses through two steps. The first step – formation of a cyclic episulfonium intermediate ion (Fig. 1) – starts with the electrophilic addition of the sulfenyl halide's sulfur atom to the π bond of the alkene. The formation of the episulfonium intermediate is known to be the rate-determining step for this reaction [4 – 15], followed by the nucleophilic *trans* attack of the halide or the hydroxide on one of the carbon atoms of the episulfonium intermediate. At low temperatures, this reaction is under kinetic control. The reaction occurs in a stereospecific anti manner, with the nucleophilic halide attacking the more substituted carbon atom, unless this carbon atom is substituted with extremely bulky groups. Most frequently the first step is reversible, so the second step determines the stereochemistry of products. The constitution of the final product depends on the nature of the substituents as well as on the reaction temperature.

The attempts to determine the most likely mechanism for electrophilic additions of sulfenyl halides

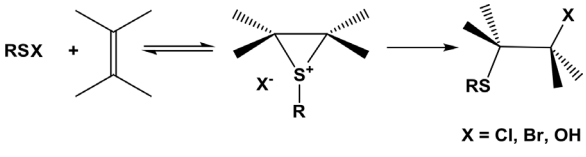

Fig 1. General scheme for the addition of sulfenyl halides to alkenes.

on the basis of frontier molecular orbital interactions [16 – 22] have shown that the final anti-addition products are obtained by the S_N2 mechanism, where the nucleophile attacks the ring carbon atoms of the episulfonium intermediate from the opposite side of the leaving group. However, the mechanism of formation of the episulfonium ions is not fully understood, and the presence of an addition complex is a matter of discussion.

Description of Methods

Quantum chemical calculations were carried out by means of the *ab initio* Hartree-Fock method using the GAMESS program [23] to study the mechanism of the reaction. We used the MP2 theory to include correlation energy corrections, inasmuch as previous reports have shown that the density functional theory for calculation of transition states is not always adequate or reliable [24 – 27]. The relevant reaction stationary points were fully optimized using the MP2/6-

31+G(d,f) level of theory calculations. We made an attempt to choose a basis set which well describes reactions with heavy atoms from the third row such as S and Cl. These atoms are essential for the reactivity of the reaction under discussion [28]. So by analogy to the computational study presented in [28] we used the 6-31+G(d,f) basis set instead of the standard 6-31+G(d,p) one.

The energy E of a molecule according to the adiabatic Born-Oppenheimer approximation consists of the electronic energy E_{elec} and the vibrational energy E_{vib}.

$$E = E_{\mathrm{elec}} + E_{\mathrm{vib}} \tag{1}$$

In order to have proper ground and transition state energies of the molecule, the electronic energies should be adjusted by vibrational zero point energies (E_0) for the initial molecules, products of reaction, intermediates, and transition states

$$E = E_{\mathrm{elec}} + E_0, \tag{2}$$

where

$$E_0 = \frac{1}{2}\sum_i \hbar\omega_i \tag{3}$$

is simply half of the summation over all the real vibrational frequencies ω_i (or vibrational energies $\varepsilon_i = \hbar\omega_i$, where $\hbar$ is the Planck constant) expressed in energy units. The scaling factor for E_0 frequencies was chosen equal to 1. All the stationary points located have been characterized as either minima or transition states (first order saddle points) by computing vibrational frequencies. Vibrational frequencies were calculated doing numerical differentiation of analytically computed MP2 gradients. The scale factors for vibrational frequencies, displacement size, as well as other quantities, were left in their default values. Transition states have a single imaginary frequency while minima have all real frequencies. Transition states have been confirmed by animating their imaginary frequency in MOLEKEL [29] and by intrinsic reaction coordinate (IRC) analysis. Visualization of the obtained structures was performed with MOLEKEL and VIEWMOL3D programs [30]. Mulliken charge distribution, bond order analysis and geometry parameters for calculated stationary points were analyzed along the reaction pathway using IRC calculation results. Thermodynamic properties were estimated under standard conditions – temperature T = 298.15 K and pressure p = 1 atm. Therefore, the translational and rotational degrees of freedom of the molecule also become important along with the vibrational degrees of freedom (Eq. 4). All of these are dependent on temperature.

$$E_{\mathrm{th}}(T) = E_{\mathrm{vib}}(T) + E_{\mathrm{trans}}(T) + E_{\mathrm{rot}}(T) \tag{4}$$

Other quantities of interest are the enthalpy H (Eq. 5) and the Gibbs Free Energy G (Eq. 6) (S = entropy, R = universal gas constant).

$$H = E_{\mathrm{el}} + E_0 + E_{\mathrm{th}}(T) + \mathrm{R}T, \tag{5}$$

$$G = H - TS \tag{6}$$

Eq. 5 is presented for one mole of molecules using the ideal gas approximation. For estimation of the studied reaction not the absolute values of G and H are important, but their differences between the initial and final state (Eqs. 7 and 8).

$$\Delta H = H_{\mathrm{fin}} - H_{\mathrm{init}} \tag{7}$$

$$\Delta G = G_{\mathrm{fin}} - G_{\mathrm{init}} \tag{8}$$

The relative Gibbs Free Energies ΔG in kcal mol^{-1} of the structures presented in Table 1 and Fig. 2 are discussed throughout the text.

Results and Discussion

In the present study we selected the electrophilic addition reaction of methylsulfenyl chloride to propene

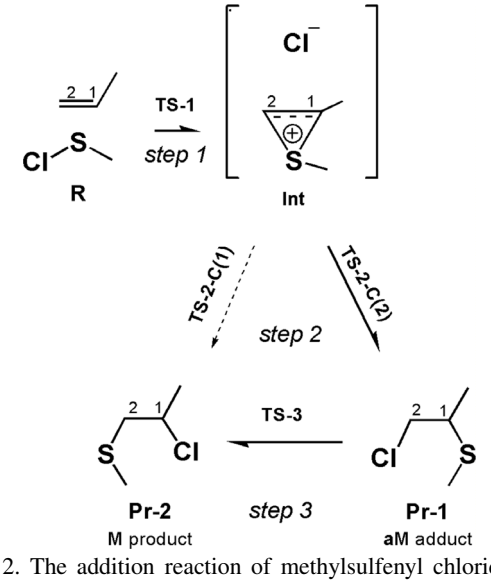

Fig 2. The addition reaction of methylsulfenyl chloride to propene.

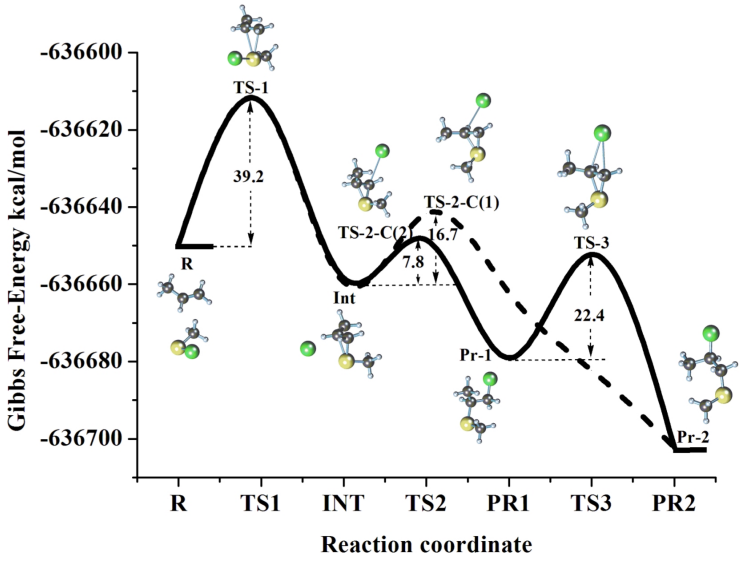

Fig. 3. The Gibbs Free Energy profile for the methylsulfenyl chloride addition to propene, with relative reaction energies presented in kcal mol^{-1}.

Table 1. The relative Gibbs Free Energies ΔG (in kcal mol^{-1}) for the stationary points of the methylsulfenyl chloride addition reaction to propene and the imaginary harmonic vibrational frequencies (IHVF) (in cm^{-1}) of the reaction transition states.

	ΔG	IHVF for TS
R	00.00	–
TS-1	39.22	306.38i
Int	−6.434	–
TS-2-C(1)	10.217	75.13i
TS-2-C(2)	1.398	76.50i
TS-3	0.280	248.70i
PR-1	−22.119	–
PR-2	−50.221	–

as a model for the theoretical study (Fig. 2). This model is the simplest possible and maintains all features of the real systems allowing a complete and efficient energy estimation to study all possible reaction routes and intermediates.

The experimental results [3 – 6, 31, 32] point to the fact that this reaction proceeds under kinetic control with a high regioselectivity. The spectroscopic and kinetic investigation of the reaction suggests that electrophilic addition of methylsulfenyl chloride to propene proceeds *via* an episulfonium intermediate followed by a nucleophilic *trans* attack of the halide on the C(2) carbon atom of the episulfonium ring to give an unstable 2-chloro anti-Markovnikoff (aM) adduct of the kinetically controlled reaction [3 – 6, 31, 32]. Upon heating the 2-chloro aM-adduct undergoes further rearrangement into a thermodynamically more stable 1-chloro Markovnikoff (M) product.

In this work we have investigated the reaction mechanism by analyzing the most probable reaction Gibbs Free Energy profiles computed at the MP2/6-31+G(d,f) level of theory. We evaluated reaction pathways proceeding under kinetic and thermodynamic control to conclusively characterize the reaction.

The progress of the methylsulfenyl chloride addition reaction to the π bond of propene can be described by three main steps: (a) the addition of methylsulfenyl chloride to the double π bond of methylethene up to the intermediate formation; (b) the regioselective episulfonium intermediate ring opening by the chloride anion, (c) the isomerization of the adduct of the kinetically controlled reaction into the thermodynamically favorable product.

A schematic sketch of the methylsulfenyl chloride addition reaction to propene is given in Fig. 2. The relative Gibbs Free Energies of the calculated stationary points and the imaginary frequencies of the transition states are presented in Table 1. The schematic Gibbs Free Energy profile for the pending reaction is presented in Fig. 3. Optimized geometries of the reactants, transition states, intermediates and the final products are displayed in Figs. 4 – 6. Intrinsic reaction coordinates (IRCs) were calculated to find the reactions' minimal energy profiles and to detail the reaction mechanism. The bond order and torsion angle changes of the reacting species are denoted in Table 2, the charge changes are presented in Table 3. These results allow us to analyze important geometrical and electronic changes on the most favorable reac-

Geometry	R	TS-1	Int	TS-2-2	Pr-1	Ts-3	Pr-2	TS-2-1
C(1)–C(2)	1.45	1.35	0.80	0.80	0.90	0.85	0.91	0.80
S–Cl	0.79	0.53	0.17	–	–	–	–	–
C(1)–Cl	–	–	0.14	−0.07	–	0.38	0.85	0.27
C(2)–Cl	–	–	0.14	0.28	0.99	0.13	–	−0.05
C(1)–S	–	0.20	0.92	0.96	0.86	0.79	0.00	0,43
C(2)–S	–	0.20	0.93	0.44	0.00	0.79	0.80	0.90
ψ	29.0	58.2	76.6	146.7	179.8	180.0	180.0	127.1

Table 2. Bond orders and Cl–C(1)–C(2)–S torsion angles (ψ in deg) for the stationary points of the methylsulfenyl chloride addition reaction to propene (the numbers of C atoms and torsion angle displacement are shown in Fig. 4).

Atom	R	TS-1	Int	TS-2-2	Pr-1	Ts-3	Pr-2	TS-2-1
C(1)	−0.123	−0.09	−0.145	−0.156	−0.192	−0.237	−0.200	−0.201
C(2)	−0.481	−0.431	−0.461	−0.505	−0.557	−0.571	−0.600	−0.511
S	+0.085	+0.411	+0.648	+0.510	+0.170	+0.545	+0.152	+0.550
Cl	−0.128	−0.542	−0,859	−0.831	−0.030	−0.764	−0.050	−0.821

Table 3. Charges on selected atoms of the stationary points of the methylsulfenyl chloride addition reaction to propene (the numbering of the C atoms is shown in Fig. 4).

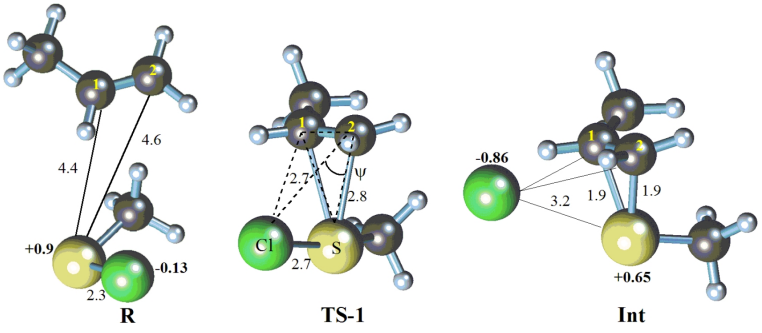

Fig. 4. Geometries and bond lengths (in Å) of the stationary points located for the step 1: the reactant **R**, the transition structure **TS-1** and the intermediate **Int**.

tion energy profile and to estimate the reaction mechanism.

The first step (step 1) of the methylsulfenyl chloride addition reaction to propene starts with the interaction of the sulfur atom and the double π bond forming two bonds S-C(1) and S-C(2) (Figs. 2 – 4). Calculations of the reaction energy profile (Fig. 3) show that the first minimum is the episulfonium intermediate **Int** followed by the transition state **TS-1**. As seen from the reaction energy profile this step is the rate-limiting step with a Gibbs activation energy of 39.22 kcal mol^{-1}. A high activation barrier for **TS-1** explains the kinetics of the episulfonium ion formation [3 – 6, 31, 32] and supports the assumption that the episulfonium ion formation is irreversible and proceeds very slowly. Moreover, the episulfonium ring formation up to **Int** is an energetically favorable stage with an energy decrease of 45.65 kcal mol^{-1}. Step 1 consists of simultaneous S–Cl bond cleavage and S–C(1) and S–C(2) bond formation to produce intermediate **Int** (Fig. 4). Thereby the sulfur atom approaches perpendicularly the olefinic double bond through the concerted transition state **TS-1**. The S–C(1) and S–C(2) bond lengths shorten from 4.4 Å (4.6 Å), and the bond orders strengthen from (BO) 0.0 for **R** to 2.7 (2.8 Å) and BO 0.2 for **TS-1**, until they reach the intermediate **Int** with the bonds length 1.9 Å and BO 0.9. Simultaneously the distance between the chloride and sulfur atoms increases. The S–Cl bonds lengthen and weaken from 2.3 Å (BO 0.8) for **R** to 2.7 Å (BO 0.5) for **TS-1** until they reach **Int** with 3.2 (BO 0.17). With this structural change the chlorine atom migrates towards the π bond. The migration of the chlorine atom was estimated by the Cl–C(1)–C(2)–S torsion angle (ψ) scan along the reaction coordinate (see Fig. 4, Table 2). The significant changes in ψ from 29.0° to 76.6° occur in this step, which indicates that as the chlorine atom migrates towards the C(1)=C(2) bond, the interaction changes from π bonding to σ bonding character. As the reacting system reaches **Int** the distances between the Cl atom and S, C(1), C(2) atoms become close to the van der Waals interaction distance, and the reactive chlorine atom is facing perpendicularly the episulfonium ring plane. This stabilizes the system, forms the episulfonium cation and the chloride anion, and leads to a decrease in energy.

At step 1 the charge of the reacting species changes, and the negative charge is transferred to the chloride atom (from −0.13 to −0.54) with a simultaneous increase of the positive charge on the sulfur atom (from +0.08 up to +0.41) as the reaction proceeds from reactant **R** to transition state **TS-1** (Table 3). The

reaction progress from **TS-1** to **Int** shows a further increase in negative charge on the chloride up to −0.86 and a reduction in electron density on the sulfur atom generating a positive charge that increases to +0.65. This charge transfer results in polarization, lengthening and weakening of the S–Cl bond up to the ionic level.

The regioselective ring opening of the episulfonium intermediate **Int** by a *trans* attack of the chloride anion is the dominating structural change at step 2 (Figs. 1 – 6). Two regioisomeric pathways are possible in this step. They proceed *via* transition states **TS-2-C(2)** and **TS-2-C(1)**. The pathway *via* **TS-2-C(2)** occurs when the chloride forms a bond with the C(2) carbon atom with simultaneous C(1)–S bond cleavage resulting in the formation of the anti-Markovnikoff (aM)-type 2-chloro derivative **Pr-1**. In the second pathway *via* **TS-2-C(1)** the chloride atom migrates towards the C(1) carbon atom resulting in the formation of the C(1)–Cl bond and the cleavage of the C(2)–S bond leading to a Markovnikoff (M)-type 1-chloro-substituted derivative **Pr-2**. The chloride anion changes its position and migrates towards the ring carbons until it reaches a position opposite to the leaving S-CH_3 group. The torsion angle expands from 76.6° for **Int** to 127.1° for **TS-2-C(1)**, and for **TS-2-C(2)** it becomes equal to 146.7°. Further reaction progress from **TS-2-C(2)** to **Pr-1** and from **TS-2-C(1)** to **Pr-2** leads to an increase of the torsion angle Cl–C(1)–C(2)–S up to 180°. Chloride forms a weak bond with C(2) and interacts repulsively with the C(1) atom when it migrates *via* the transition state **TS-2-C(2)**. At this stage the C(2)–Cl distance shortens, and the bond strengthens from 3.4 Å (BO 0.14) for **Int** to 3.0 Å (BO 0.3) for **TS-2-C(2)**, while the C(1)–Cl distance increases to 3.5 Å with a negative BO value of −0.1 indicating repulsive interactions between C(1) and Cl. In contrast, the transition state **TS-2-C(1)** stabilizes the bonding interaction between the C(1) and Cl atoms at a distance of 3.0 Å (BO 0.3) and the repulsive interaction between C(2) and Cl with a BO value of −0.1. The bond lengths and BOs of the S–C(1) and S–C(2) bonds at this step remain unchanged 1.9 Å (BO 0.8).

This step has a low activation barrier. For the episulfonium ring opening reaction the Gibbs activation energies of **TS-2-C(2)** and **TS-2-C(1)** are 7.83 and 16.65 kcal mol^{-1}, respectively, starting from intermediate **Int**. Thus **TS-2-C(2)** is lower in energy than **TS-2-C(1)** by 8.82 kcal mol^{-1}. This energy difference appears to be due to a steric effect between the bulky

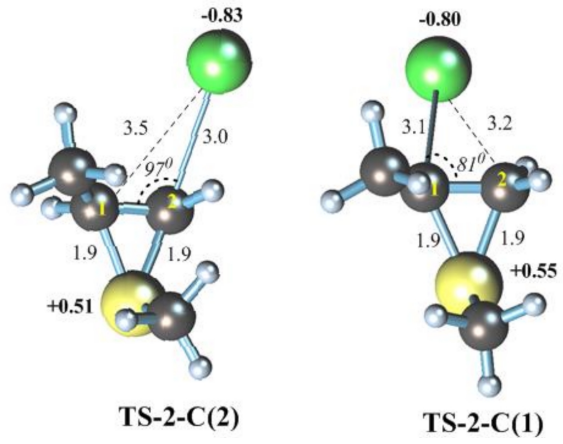

Fig. 5. Geometries, charges and bond lengths (in Å) of the stationary points located for the step 2: the transition structures **TS-2-C(1)**, **TS-2-C(2)**.

methyl group and the chlorine atom [33]. As presented in Fig. 5 the angle Cl–C(1)–C(2) for **TS-2-C(1)** is equal to 81° and is close to the opened Cl–C(1)–C(2) angle of 97° for **TS-2-C(2)**. It shows that the attack of the chlorine on the C(1) atom is more hindered due to the steric effect of the methyl group. Thus it may be conceived that at first the 2-chloro adduct **Pr-1** is formed owning to its low activation energy. This result is in accordance with experiments [3 – 6, 31, 32] which suggest that the primarily kinetically controlled reaction proceeds to the unstable 2-chloro adduct **Pr-1**.

Moreover, the calculated low activation barriers of step 2 are compatible with our earlier theoretical results [25, 26]. There it was pointed out that the chloride anion attack on either C(1) or C(2) carbon atoms of the thiiranium ion is to be taken as the frontier molecular orbitals controlled reaction. The regioselectivity features of the thiiranium ion ring-opening reaction by the chloride anion is governed by the small energy gap between the LUMO (lowest unoccupied molecular orbital) and LUMO+1 of the intermediate, as well as by the shape distribution of these LUMO's and the HOMO (highest occupied molecular orbital) of the approaching chloride anion [25, 26]. The results can be explained using the Leffler Hammond postulate [34 – 36], which states that the minor energy changes of the reacting species in a reaction PES correspond to the minor changes in the geometry and electronic structure of these species. So, the closeness in energy of the reaction intermediate **Int** and transition states **TS-2-C(2)** and **TS-2-C(1)** of the *step 2* corresponds to the minor changes of their geometry

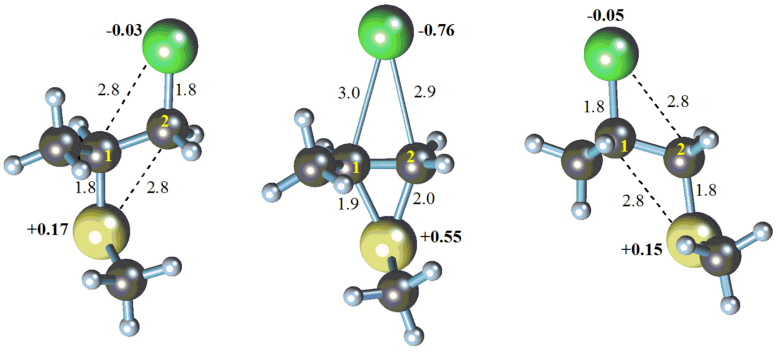

Fig. 6. Geometries, charges and bond lengths (in Å) of the stationary points located for the step 3: the transition structure **TS-3** and the products **Pr-1**, **Pr-2**.

and electronic structure. Therefore the influence of the electronic structure of the thiiranium intermediate **Int** reflects well the regioselectivity features of the reaction.

The charge transfer scan on the reaction coordinate shows that, as the reaction proceeds from **TS-2-C(1)** to product **Pr-1** and from **TS-2-C(2)** to **Pr-2**, the electron density on the chloride anion is transferred to the sulfur atom. The positive charge on sulfur is reduced from $+0.51$ to $+0.17$ with a negative charge decrease on the chloride from -0.83 to -0.03.

As pictured in Fig. 3 and shown in Table 1 the final reaction product **Pr-2** is by 28.1 kcal mol^{-1} less in energy than the initial adduct **Pr-1**. The energy difference between **Pr-1** and **Pr-2** represents the difference in thermodynamic stability of these isomers and suggests the possibility of a reaction pathway for the 2-chloro adduct **Pr-1** of the kinetically controlled reaction to a more energetically favorable 1-chloro product **Pr-2**. The reaction energy profile for step 3 shows that the isomerization reaction goes *via* transition state **TS-3** with an activation barrier of 22.4 kcal mol^{-1} to a more stable product **Pr-2**. The values for the reaction energy profile reveal the possibility of isomerization *via* transition state **TS-3**, which extends to the experimental observations. The experimental findings [3–6, 31, 32] on the reaction kinetics show that the isomerization reaction proceeds *via* a transition state with the reaction rate constant value different from the rate constant value specific for the formation of the episulfonium ion. This suggests that the isomerization reaction is not reversed through the episulfonium intermediate.

At step 3 the angle ψ for transition state **TS-3** and products **Pr-1** and **Pr-2** remains unchanged and is equal to 180°, while the Cl-C(2) and Cl-C(1) bonds lengths increase from 1.9 to 2.9 Å during the isomerization process.

A negative charge transfer to the chloride atom from -0.03 to -0.76 simultaneously causes a positive charge distribution on the sulfur atom from $+0.17$ up to $+0.55$ while the reaction proceeds from **Pr-1** to **TS-3**. A further charge transfer occuring as the reaction progresses to **Pr-2** is opposite. A high negative charge on the chloride anion is transferred to the sulfur atom thereby reducing the positive charge on the sulfur atom from $+0.55$ to $+0.15$ with a decrease in negative charge on the chloride to -0.05.

Thus, our computational results support the experimental kinetic and spectroscopic studies [3–6, 31–32]. They confirm that the ring closure step is the rate-limiting step for the addition reaction leading to the formation of the episulfonium cation as the reaction intermediate. The episulfonium intermediate ring formation step has the highest energy barrier. The regioselective episulfonium intermediate ring opening reaction further proceeds on two possible regioisomeric pathways. Our calculations show that the intermediate ring-opening process proceeds firstly by the chloride anion attack to C(2) carbon *via* **TS-2-C(2)**, forming an unstable 2-chloro addition adduct **Pr-1** of the kinetically controlled reaction. Finally the isomerization reaction of the adduct **Pr-1** proceeds *via* transition state **TS-3** to form a thermodynamically stable product **Pr-2**.

[1] G. K. Helmkamp, D. J. Pettitt, *J. Org. Chem.* **1960**, *25*, 1754.

[2] G. K. Helmkamp, D. J. Pettitt, *J. Org. Chem.* **1962**, *27*, 2942.

[3] A. T. Warren, *J. Org. Chem*. **1969**, *34*, 871.
[4] W. H. Mueller, *Angew. Chem*. **1969**, *81*, 475; *Angew. Chem., Int. Ed. Engl.* **1969**, *8*, 482.
[5] A. Vektariene, *Pharm. Chem. J.* **1998**, *32*, 629.
[6] L. Rasteikiene, D. Greiciute, M. G. Linkova, I. L. Knunyants, *Rus. Chem. Rev*. **1977**, *46*, 548.
[7] H. Liu, I. P. Smoliakova, L. N. Koikov, *Org. Lett.* **2002**, *4*, 3895.
[8] I. P. Smoliakova, *Current Org. Chem*. **2000**, *4*, 589.
[9] T. Dudley, I. Smoliakova, M. Hoffmann, *J. Org. Chem*. **1999**, *64*, 1247.
[10] B. D. Johnson, B. M. Pinto, *J. Org. Chem*. **2000**, *65*, 4607.
[11] C. Baldwin, P. Briner, M. D. Eastgate, D. J. Fox, S. Warren, *Org. Lett*. **2002**, *4*, 4381.
[12] I. A. Abu-Yousef, R. C. Hynes, D. N. Harp, *Tetrahedron Lett.* **1993**, *34*, 4289.
[13] D. K. Jones, D. C. Liotta, *Tetrahedron Lett*. **1993**, *34*, 7209.
[14] D. Fox, D. House, *Angew. Chem*. **2002**, *114*, 2572; *Angew. Chem. Int. Ed.* **2002**, *41*, 2462.
[15] P. Bird, J. Eames, A. G. Fallis, R. V. H. Jones, M. Roddis, C. F. Sturino, S. O'Sullivan, S. Warren, M. S. Westwell, J. Worrall, *Tetrahedron Lett.* **1995**, *36*, 1909.
[16] Y. Kukuzono, T. Yamabe, S. Nagata, H. Kato, K. Fukui, *Tetrahedron* **1974**, *30*, 2197.
[17] A. Vektariene, G. Vektaris, D. W. H. Rankin, *Heteroatom Chem.* **2007**, *18*, 695.
[18] G. Modena, L. Pasquato, V. Lucchini, *Chem. Eur. J.* **2000**, *6*, 589.
[19] V. Lucchini, G. Modena, L. Pasquato, *J. Am. Chem. Soc.* **1993**, *115*, 4527.
[20] G. Capozzi, V. Lucchini, G. Modena, *Res. Chem. Intermed*. **1979**, *4*, 347.
[21] V. Lucchini, G. Modena, L. Pasquato, *J. Am. Chem. Soc.* **1995**, *117*, 2297.
[22] a) M. Fachini, V. Lucchini, G. Modena, M. Pasi, L. Pasquato, *J. Am. Chem. Soc.* **1999**, *121*, 3944; b) A. Vektariene, G. Vektaris, *Arkivoc* **2006**, *16*, 23.
[23] M. W. Schmidt, K. K. Baldridge, J. A. Boatz, S. T. Elbert, M. S. Gordon, J. H. Jensen, S. Koseki, N. Matsunaga, K. A. Nguyen, S. Su, T. L. Windus, M. Dupuis, J. A. Montgomery, *J. Comput. Chem.* **1993**, *14*, 1347
[24] I. Díaz-Acosta, J. R. Alvarez-Idaboy, A. Vivier-Bunge, *Int. J. Chem. Kinet.* **1999**, *31*, 29.
[25] J. R. Alvarez-Idaboy, I. Diaz-Acosta, A. Vivier-Bunge, *J. Comput. Chem.*, **1998**, *19*, 811.
[26] H. Uc, I. García-Cruz, A. Hernández-Laguna, A. Vivier-Bunge, *J. Phys. Chem. A*, **2000**, *104*, 7847.
[27] V. H. Uc, I. García-Cruz, A. Vivier-Bunge, *Quantum Systems in Chemistry and Physics*, Vol. 2, *Advanced Problems and Complex Systems*, Kluwer Academic Publishers, London, **2000**, p. 241.
[28] S. Perreault, M. Poirier, P. Leveille, O. Rene, P. Joly, Y. Dory, C. Spino, *J. Org. Chem.* **2008**, *73*, 7457.
[29] P. Flukiger, H. P. Luthi, S. Portmenn, J. Weber, MOLEKEL 4.3, Swiss Center for Scientific Computing, Manno (Switzerland) **2000**
[30] A. Ryzhkov, A. Antipin, VIEWMOL3D, Program for Visualization of Molecules Models: http://redandr.ca/vm3/.
[31] W. H. Mueller, P. E. Butler, *J. Am. Chem. Soc*. **1968**, *90*, 2075.
[32] W. A. Thaler, W. H. Mueller, P. E. Butler, *J. Am. Chem. Soc*. **1968**, *90*, 2069.
[33] T. Fujita, C. Takayama, M. Nakajima, *J. Org. Chem*. **1973**, *38*, 1623.
[34] A. Yarnell, *Chemical & Engineering News* **2003**, *81*, 42.
[35] J. E. Leffler, *Science* **1952**, *117*, 340.
[36] G. S. Hammond, *J. Am. Chem. Soc.* **1953**, *77*, 334.